

# High-Resolution Solid State $^{19}\text{F}$ and $^{15}\text{N}$ MAS NMR Spectra of Fluoroaromatics and Aromatic Nitrogen Heterocycles Physisorbed on Silica and Alumina

Gero von Fircks, Heike Hausmann, Volkhard Francke, and Harald Günther\*

Fachbereich 8, OC II, University of Siegen, D-57068 Siegen, Germany

Received June 12, 1996 (Revised Manuscript Received May 7, 1997<sup>o</sup>)

High-resolution  $^{19}\text{F}$  and  $^{15}\text{N}$  solid state MAS NMR spectra have been obtained for fluoro-substituted aromatics and for aromatic nitrogen heterocycles, respectively, adsorbed on silica and alumina, where line narrowing is due to the high mobility of these systems on the surface of the porous materials.  $^{19}\text{F}$ ,  $^{19}\text{F}$  COSY,  $^{19}\text{F}$ ,  $^{13}\text{C}$  HETCOR, and  $^{19}\text{F} \rightarrow ^{13}\text{C}$  INEPT experiments were successfully performed, and  $^{15}\text{N}$  NMR was measured in natural abundance.

## Introduction

Solid state NMR has emerged as a valuable tool in the study of adsorption phenomena,<sup>1</sup> and many liquids and gases are highly mobile when physisorbed on silica,<sup>1a</sup> zeolites,<sup>1a,c</sup> graphite,<sup>1b</sup> or boron nitride.<sup>1b,2</sup> As a consequence, line-narrowing is found in solid state NMR spectra of adsorbed molecules like olefins, methylated and other substituted benzenes, or pyridine.<sup>1</sup>

Recently we have shown that high-resolution  $^{13}\text{C}$  and  $^1\text{H}$  solid state NMR spectra can also be observed for hydrocarbons like naphthalene or phenanthrene with the magic-angle-spinning (MAS) technique already at moderate spinning speeds of 2 kHz and less if these systems are physisorbed on porous materials like alumina or silica.<sup>3</sup> Due to the high mobility of the physisorbed species on the surface of the adsorbents, phenomena that cause line broadening typical for NMR of solids, like dipolar interactions and chemical shift anisotropies,<sup>4</sup> are further reduced and  $^{13}\text{C}$  spectra with line widths on the order of 10–30 Hz result. Even the observation of individual proton resonances becomes possible, the line widths being here roughly 1 order of magnitude larger. In line with these observations is the finding that  $^1\text{H}$ ,  $^{13}\text{C}$  cross polarization (CP), which rests on dipolar  $^1\text{H}$ ,  $^{13}\text{C}$  coupling, fails and the spectra of the adsorbed aromatics have to be recorded under MAS conditions with direct  $^{13}\text{C}$  excitation. Another aspect of general interest that emerged from our study is that adsorption can be initiated by a simple grinding procedure, even though an inhomogeneous distribution of the adsorbates on the silica surface results<sup>5,6</sup> (see also below and Experimental Section).

In view of the attention paid presently to surface phenomena,<sup>7,8</sup> and with respect to their importance in catalytic processes,<sup>7</sup> a straightforward extension of our investigations to other nuclei was desirable in order to evaluate the influence of adsorption on the respective NMR spectra.  $^{19}\text{F}$  and  $^{15}\text{N}$  were obvious candidates for such a study, the former because of the strong homo- and heteronuclear dipolar interactions which exist in perfluorinated compounds and fluorinated hydrocarbons,<sup>9,10</sup> respectively, and the latter because of its low natural abundance (0.36%). In fact, the majority of  $^{15}\text{N}$  solid state NMR investigations performed so far have been on labeled material.<sup>5,11–17</sup>

## Results and Discussion

**$^{19}\text{F}$  Measurements.** Samples were prepared as described<sup>3</sup> by grinding the organic material with alumina or silica—which was not subjected to any pretreatment and therefore contained various amounts of surface water<sup>18</sup>—in an agate mortar (cf. Experimental Section). Decafluorobiphenyl (**1**), 3-fluorophenanthrene (**2**), 1-, 2-, and 9-fluoroanthracene (**3**, **4**, **5**), as well as 1- and 2-fluoroanthraquinone (**6**, **7**) served for the  $^{19}\text{F}$  measurements (Chart 1). Figure 1 shows the  $^{19}\text{F}$  MAS NMR spectra obtained for samples of **1–4** and **7** adsorbed on silica 60; the complete data are collected in Table 1.  $^1\text{H}$  decoupling could not be applied because the  $^1\text{H}$  coil of

(7) See, for example: *Characterization of Porous Materials II, Studies in Surface Science and Catalysis*, Vol. 62; Rodriguez-Reinoso, F., Rouquerol, J., Sing, K. S. W., Unger, K. K., Eds.; Elsevier: Amsterdam, 1991.

(8) *Preparative Chemistry Using Supported Reagents*; Laszlo, P., Ed.; Academic Press: New York, 1987.

(9) Harris, R. K.; Jackson, P. *Chem. Rev.* **1991**, *91*, 1427.

(10) Carss, S. A.; Scheler, U.; Harris, R. K., Holstein, P.; Fletton, R. A. *Magn. Reson. Chem.* **1996**, *34*, 63.

(11) Bernstein, T.; Kitaev, L.; Michel, D.; Pfeifer, H.; Fink, P. *J. Chem. Soc., Faraday Trans. 1* **1982**, *78*, 237.

(12) Michel, D.; Germanus, A.; Pfeifer, H. *J. Chem. Soc., Faraday Trans. 1* **1982**, *78*, 237.

(13) Maciel, G. E.; Haw, J. F.; Chuang, I.-S.; Hawkins, B. L.; Early, T. A.; McKay, D. R.; Petrakis, L. *J. Am. Chem. Soc.* **1983**, *105*, 5529.

(14) Haw, J. F.; Chuang, I.-S.; Hawkins, B. L.; Maciel, G. E. *J. Am. Chem. Soc.* **1983**, *105*, 7206.

(15) Ripmeester, J. A. *J. Am. Chem. Soc.* **1983**, *105*, 2925.

(16) Majors, P. D.; Ellis, P. D. *J. Am. Chem. Soc.* **1987**, *109*, 1648.

(17) Smith, J. A. S.; Wehrle, B.; Aguilar-Parrilla, F.; Limbach, H.-H.; Foces-Foces, M. C.; Cano, F. H.; Elguero, J.; Baldy, A.; Pierrot, M.; Khurshid, M. M. T.; Larcombe-McDouall, J. B. *J. Am. Chem. Soc.* **1989**, *111*, 7304.

(18) Thermogravimetric measurements gave a surface water content of ca. 5% (Francke, V. Diploma thesis, University of Siegen, 1995), which corresponds to the concentration found for silica stored at room temperature at "normal" humidities.

\* Abstract published in *Advance ACS Abstracts*, June 15, 1997.

(1) (a) Pfeifer, H.; Meiler, W.; Deininger, D. *Ann. Rep. NMR Spectrosc.* **1983**, *15*, 291. (b) Boddenberg, B. *Lectures on Surface Science*; Castro, G. R., Cardona, M., Eds.; Springer: Berlin 1987. (c) Engelhardt, G.; Michel, D. *High-Resolution Solid State NMR of Silicates and Zeolites*; Wiley: Chichester, 1987. (d) Ansermet, J.-Ph.; Slichter, C. P.; Sinfelt, J. H. *Progr. NMR Spectrosc.* **1990**, *22*, 401. (e) Nagy, J. B. *NATO Asi Ser. C* **1990**, *322*, 371.

(2) Grosse, R.; Boddenberg, B. *Z. Phys. Chem. N.F.* **1987**, *152*, 1.

(3) Ebener, M.; von Fircks, G.; Günther, H. *Helv. Chim. Acta* **1991**, *74*, 1296.

(4) (a) Fyfe, C. A. *Solid State NMR for Chemists*; CFC Press: Guelph, 1983. (b) Grimmer, A.-R.; Blümich, B. *NMR - Basic Principles and Progress*; Diehl, P., Kosfeld, R., Fluck, W., Günther, H., Seelig, J., Eds.; Springer: Berlin, 1994; Vol. 30, p 1.

(5) Aguilar-Parrilla, F.; Claramunt, R. M.; López, C.; Sanz, D.; Limbach, H.-H.; Elguero, J. *J. Phys. Chem.* **1994**, *98*, 8752.

(6) Oepen, S. B.; Günther, H., unpublished. Oepen, S. B. Ph.D. Thesis, University of Siegen, 1996.

Chart 1

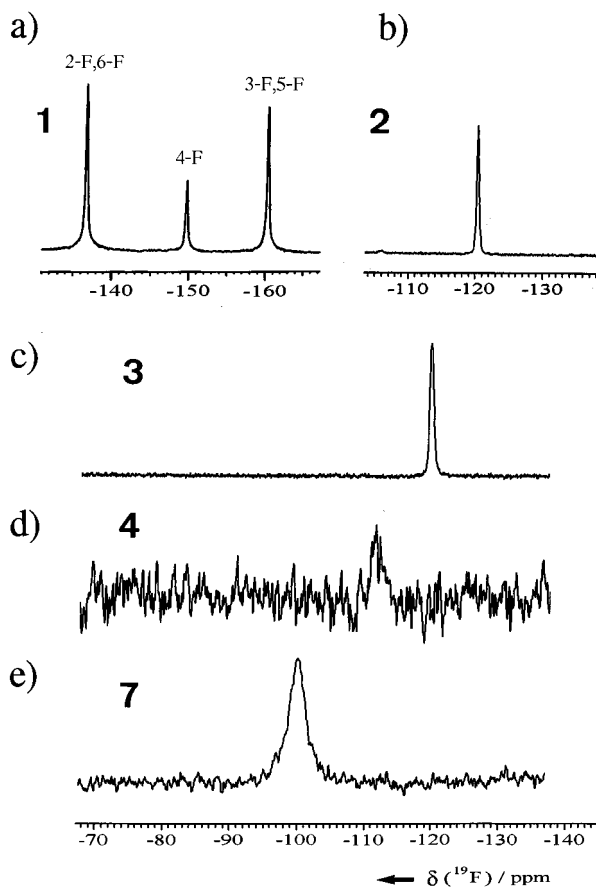
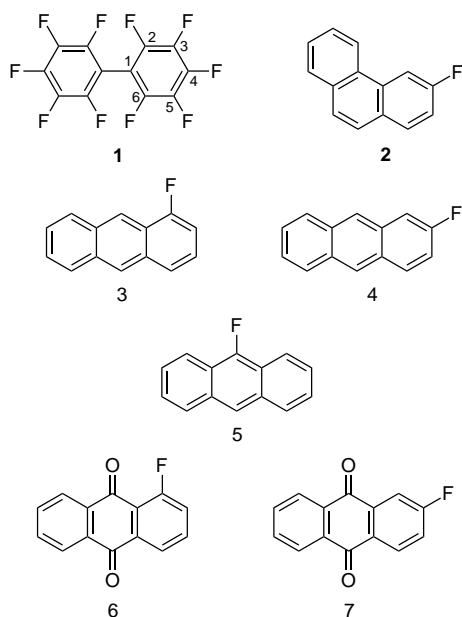


**Figure 1.** Typical examples of 282.4 MHz  $^{19}\text{F}$  MAS NMR spectra of fluorinated aromatics adsorbed on silica 60 (1:10 w/w),  $T = 292$  K, rotational frequency 4 kHz: (a) decafluorobiphenyl (**1**); (b) 3-fluorophenanthrene (**2**); (c) 1-fluoroanthracene (**3**); (d) 2-fluoroanthracene (**4**); (e) 2-fluoroanthraquinone (**7**).  $\delta$  scale relative to  $\text{C}^{19}\text{FCl}_3$  (cf. Experimental Section). Spectra b–e were recorded without  $^1\text{H}$  decoupling (cf. Experimental Section).

the probehead was tuned to the  $^{19}\text{F}$  frequency and the X coil had a limited X-frequency range (40–122 MHz) (cf. Experimental Section). Relatively sharp  $^{19}\text{F}$  signals are observed for **1–3** and **5** (not shown), while considerable

**Table 1.**  $^{19}\text{F}$  Chemical Shifts ( $\delta$ , ppm, Relative to External  $\text{C}^{19}\text{FCl}_3$ ), Half-Width  $\Delta$  (Hz), and Melting Points ( $^\circ\text{C}$ ) of Fluoroaromatics 1–7

	$\delta(^{19}\text{F})$ on silica	$\delta(^{19}\text{F})$ in $\text{CDCl}_3$	$\Delta\delta^a$	$\Delta^b$	mp, $^\circ\text{C}$
<b>1</b> $\text{F}_{\text{ortho}}$	-136.9	-136.2	-0.7	127	67
$\text{F}_{\text{meta}}$	-160.7	-159.0	-1.7	153	
$\text{F}_{\text{para}}$	-150.1	-148.5	-1.6	170	
<b>2</b>	-110.1	-114.7	4.6	122	87
<b>3</b>	-119.4	-123.7	4.3	197	109
<b>4</b>	-111.3	-115.4	4.1	~700	219
<b>5</b>	-130.6	-132.3	1.7	140	103
<b>6</b>	-112.8	-112.1	-0.7	1800	228
<b>7</b>	-99.6	-102.9	3.3	791	197

$^a \delta(^{19}\text{F})_{\text{silica}} - \delta(^{19}\text{F})_{\text{CDCl}_3}$ .  $^b$  Line width.

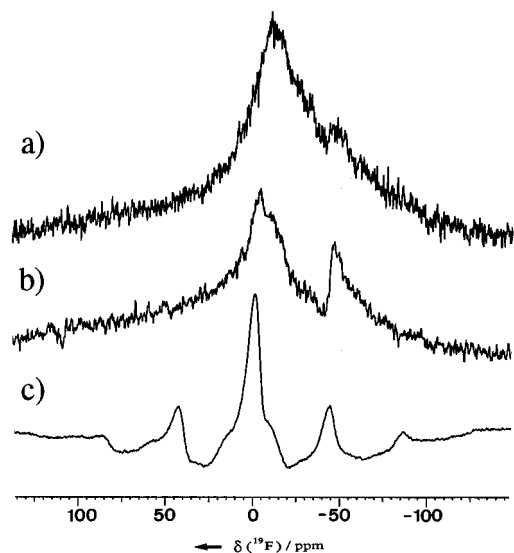


**Figure 2.** 282.4 MHz  $^{19}\text{F}$  MAS NMR spectra of crystalline 1-fluoroanthracene (**3**) (a) and 2-fluoroanthracene (**4**) (b) at 292 K and 4 kHz spinning speed. (c) The spectrum of **3** at 12 kHz spinning speed.

broader signals are found for **4**, **6**, and **7** (Figure 1 and Table 1). However, as demonstrated by comparison to Figure 2, which shows  $^{19}\text{F}$  MAS NMR spectra of crystalline **3** and **4**, the effects of homonuclear  $^{19}\text{F}$ ,  $^{19}\text{F}$  as well as heteronuclear  $^1\text{H}$ ,  $^{19}\text{F}$  dipolar coupling and of chemical shift anisotropy are largely eliminated in the spectra of the adsorbed materials. Even higher spinning rates for the crystal powder sample yielded broad lines (3.2 kHz) and a side band pattern (Figure 2c). Homonuclear scalar  $^{19}\text{F}$ ,  $^{19}\text{F}$  coupling constants in **1** and heteronuclear scalar  $^1\text{H}$ ,  $^{19}\text{F}$  coupling constants in **2–7** are on the order of 20 Hz and are not resolved in the spectra of the adsorbed systems.

Upon adsorption, there are small low- and high-frequency shifts for the  $^{19}\text{F}$  resonances (Table 1), which, however, do not exceed 5 ppm. When the large  $^{19}\text{F}$  chemical shift range is considered, no significance can presently be attached to this finding, especially since the observed effects are within the error limits of the reproducibility achieved with the grinding procedure which was used for adsorption. However, as found earlier,<sup>3</sup> there is a parallel behavior between the line widths and the melting points of the adsorbed compounds. Adsorption and mobility are apparently reduced for higher melting systems which leads to stronger line broadening, attributable primarily to residual dipolar coupling and chemical shift anisotropy effects. This correlation is particularly striking for the structurally

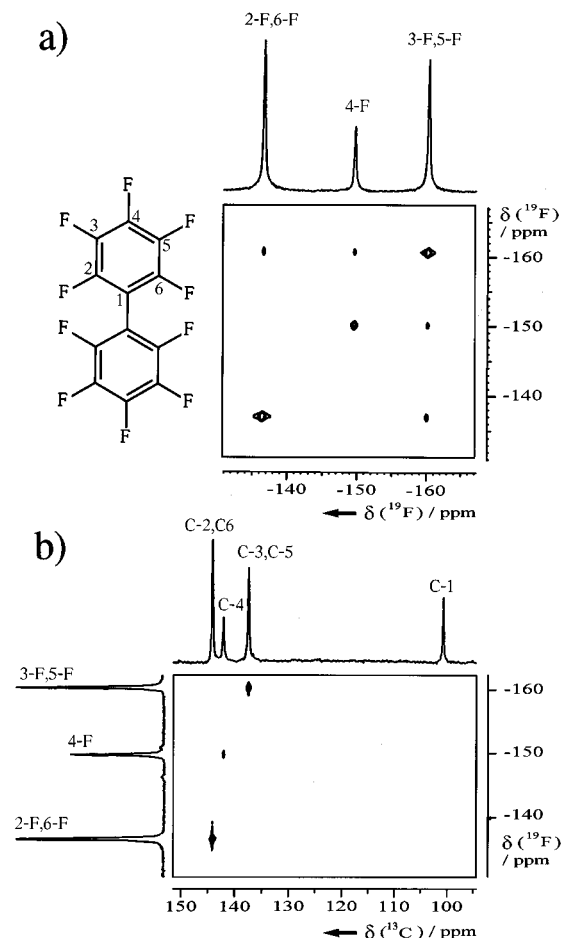


**Figure 3.** (a)  $^{19}\text{F}$ ,  $^{19}\text{F}$  COSY spectrum of **1** adsorbed on silica 60 (1:10 w/w) recorded with the standard  $90^\circ$ ,  $t_1$ ,  $90^\circ$ ,  $t_2$  COSY sequence. (b)  $^{13}\text{C}$ ,  $^{19}\text{F}$  shift correlation for **1** recorded with the standard HETCOR sequence.<sup>22</sup>

related fluoroanthracenes **3–5** (Table 1). However, a quantitative relation between the NMR behavior and the melting point cannot be formulated, and cases which are at variance with such a generalization have been found.<sup>19</sup>

**Homo- and Heteronuclear 1D and 2D Experiments for Structure Analysis.** With respect to surface reactions, structural studies of physisorbed compounds are important and the successful applications of 2D techniques for adsorbed species<sup>3,19–21</sup> are thus of general interest. We therefore tested a number of 1D and 2D experiments available for these type of investigations also for the fluorinated systems. Figure 3 shows that homonuclear  $^{19}\text{F}$ ,  $^{19}\text{F}$  COSY spectroscopy as well as heteronuclear  $^{13}\text{C}$ ,  $^{19}\text{F}$  shift correlations (HETCOR spectra<sup>22</sup>) is feasible. As in similar cases with broadened resonance signals,<sup>23</sup> cross peaks are clearly observed in the COSY spectrum even if line splittings in the 1D spectrum are not resolved.

In the case of **2**, long-range  $^{13}\text{C}$ ,  $^{19}\text{F}$  correlations based on geminal and vicinal  $^{13}\text{C}$ ,  $^{19}\text{F}$  coupling constants were successfully detected by 1D  $^{19}\text{F} \rightarrow ^{13}\text{C}$  INEPT<sup>24</sup> experiments. Figure 4 shows part of the  $^{13}\text{C}$  NMR spectrum of

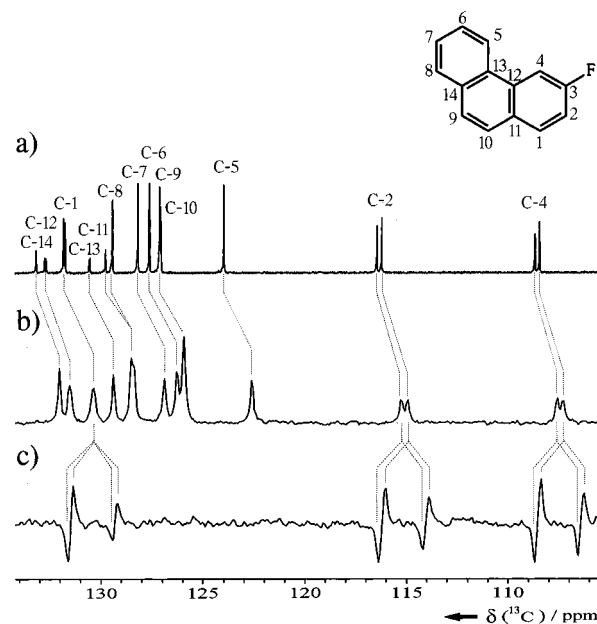


**Figure 4.** (a) 75 MHz  $^{13}\text{C}\{^1\text{H}\}$  NMR spectrum of **2**, 0.1 mol in acetone- $d_6$ ; the doublet of C-3 ( $^1J(^{13}\text{C}, ^{19}\text{F}) = 243.7$  Hz) at 162.5 ppm is not shown ( $\delta$  scale relative to TMS); for the resonance assignment, see Experimental Section,  $\delta$  values are given in Table 4). (b) 75.5 MHz  $^{13}\text{C}\{^1\text{H}\}$  MAS NMR spectrum of **2** adsorbed on alumina 90 (neutral, 1:10 w/w). (c) Long-range  $^{19}\text{F} \rightarrow ^{13}\text{C}$  INEPT<sup>24</sup> spectrum of **2** (adsorbed on alumina 90, neutral, 1:10 w/w), optimized for  $J(^{13}\text{C}, ^{19}\text{F}) = 20$  Hz;  $^1\text{H}$  coupled.

**Table 2.**  $^{13}\text{C}$ ,  $^{19}\text{F}$  and One-Bond  $^{13}\text{C}$ ,  $^1\text{H}$  Coupling Constants (Hz) for **2**

	solution <sup>a</sup>	adsorbed <sup>b</sup>		adsorbed <sup>b</sup>
C-1,F	9.0	11.1	C-1,H	160.9
C-2,F	24.1	25.0	C-2,H	163.7
C-4,F	22.5	22.2	C-4,H	160.9
C-3,F	243.7	241.4		

<sup>a</sup> Acetone- $d_6$ ,  $\pm 0.4$  Hz. <sup>b</sup> Neutral  $\text{Al}_2\text{O}_3$ .

**2** in solution and adsorbed on neutral alumina. A systematic high-field shift of 1.0–1.5 ppm is observed for the adsorbed species, which is, however, most probably due to a systematic error introduced by the indirect reference method used (see Experimental Section). The large  $^2J(^{13}\text{C}, ^{19}\text{F})$  coupling constants for C-2 and C-4 (ca. 20 Hz) are clearly resolved in both spectra, and the data are practically identical (Table 2). In the INEPT spectrum (Figure 4c) the resonances of C-2, C-4, and C-1 are excited by polarization transfer from the  $^{19}\text{F}$  nucleus and are additionally split by the one-bond  $^{13}\text{C}$ ,  $^1\text{H}$  coupling, because during the INEPT experiment proton decoupling could not be applied (cf. above and Experimental Section). The high intensity of the low-field antiphase doublet for C-1 indicates that also C-12, which is not coupled to a directly attached proton, has been excited by an INEPT transfer over three bonds.

**$^{15}\text{N}$  Measurements.** Several studies on pyridine adsorbed on alumina,<sup>15,16</sup> silica-alumina,<sup>13,15</sup> or in the cavity of zeolites<sup>11,12</sup> have been performed which were based on  $^{15}\text{N}$ -labeled material. Similarly, a recent study of pyrazole and 3,5-dimethylpyrazole adsorbed on silica or alumina<sup>5</sup> used  $^{15}\text{N}$ -labeled compounds. For our natural abundance studies we chose quinazoline (**8**, mp 45 °C), quinoline-3-carbonitrile (**9**, mp 105 °C), and quinoxaline (**10**, mp 30 °C).

(25) Levy, G. C.; Lichter R. L. *Nitrogen-15 NMR Spectroscopy*; Wiley-Interscience: New York, 1979.

(19) Ebener, M. Ph.D. Thesis, University of Siegen, 1994.  
 (20) Schwark, U.; Michel, D. *Z. Phys. Chem.* **1995**, *189*, 29.  
 (21) von Fircks, G. Ph.D. Thesis, University of Siegen, 1995.  
 (22) Bodenhausen, G.; Freeman, R. *J. Magn. Reson.* **1977**, *28*, 471.  
 (23) (a) Günther, H.; Moskau, D.; Dujardin, R.; Maercker, A. *Tetrahedron Lett.* **1986**, *27*, 2251. (b) Moskau, D.; Günther, H. *Angew. Chem.* **1987**, *99*, 151; *Angew. Chem., Int. Ed. Engl.* **1987**, *26*, 156.  
 (24) Morris, G. A.; Freeman, R. *J. Am. Chem. Soc.* **1979**, *101*, 760.

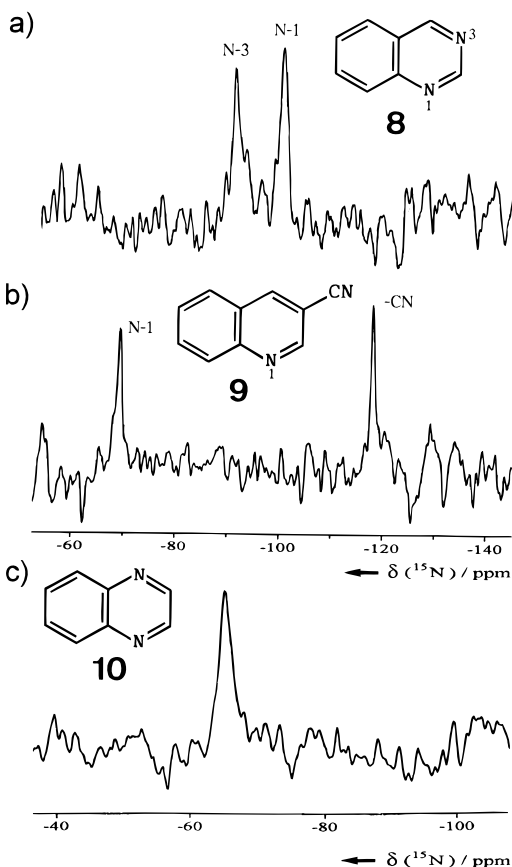


**Figure 5.** 30.4 MHz natural abundance  $^{15}\text{N}\{^1\text{H}\}$  MAS NMR spectra of **8** (a), **9** (b), and **10** (c) adsorbed on  $\gamma\text{-Al}_2\text{O}_3$  (neutral, 1:5 w/w); rotational frequency 4 kHz;  $\delta$  scale relative to  $\text{CH}_3\text{-NO}_2$ : (a)  $T = 291$  K, 2000 scans, relaxation delay 5 s, expt time 2.8 h; (b)  $T = 320$  K, 1600 scans, relaxation delay 15 s, expt time 6.6 h; (c)  $T = 293$  K, 2000 scans, relaxation delay 3 s, expt time 1.7 h.

Already the  $^{13}\text{C}$  MAS NMR spectra of **8** and **9** adsorbed on neutral alumina indicated high mobility. An elevated temperature (320 K) was used for the measurements of **9** because we had found that this can lead to additional line narrowing.<sup>19</sup> The  $^{13}\text{C}$  line widths are slightly larger (110 Hz for **8** and 70 Hz for **9**) than those found for hydrocarbons (10–30 Hz)<sup>3</sup> and splittings due to one-bond  $^{13}\text{C}, ^1\text{H}$  coupling were not resolved in  $^{13}\text{C}$  MAS spectra recorded with  $^1\text{H}$  coupling because of line broadening due to long-range spin–spin interactions and strong signal overlap. Nevertheless, satisfactory  $^{13}\text{C}$  resolution was obtained and the chemical shift data, which are collected in Table 4 and in the Experimental Section, differ only insignificantly from the solution data.

Not unexpectedly then, the  $^{15}\text{N}$  MAS NMR spectra of **8–10** yielded a sufficient signal-to-noise ratio after 2000 and 1600 transients (Figure 5), where an elevated temperature was again used during the measurements in the case of **9**. The chemical shifts and the line widths are given in Table 3. Again, the small shift differences between the data from solution measurements and those from the adsorbed species are not significant. Their magnitude is well below the shift which would result if nitrogen protonation at acidic sites of the adsorbent had occurred. For protonation, shifts of 100 and 50 ppm were reported for pyridine<sup>26</sup> or pyrimidine,<sup>27</sup> respectively, in solution. For weak hydrogen bonds, shift differences on the order of 10–12 ppm are found if chloroform is replaced by methanol.<sup>26</sup> Pyridine adsorbed on silica–

**Table 3.**  $^{15}\text{N}$  Chemical Shifts of Nitrogen Heterocycles **8–10** in Solution (A), Adsorbed on Neutral  $\text{Al}_2\text{O}_3$  (B), in the Crystal (C), and on Acidic (E) and Basic (F) Alumina ( $\delta$  Values in ppm Relative to External  $\text{CH}_3\text{NO}_2$ )

	A <sup>a</sup>	B <sup>b</sup>	C <sup>c</sup>	D <sup>d</sup>	E <sup>e</sup>	F <sup>f</sup>
<b>8</b> N-1	-99.0 <sup>g</sup>	-100.8	<i>h</i>	-1.8	-100.4	-100.2
N-3	-88.3 <sup>g</sup>	-91.4	<i>h</i>	-3.1	-90.6	-91.4
<b>9</b> N-1	-65.8	-69.3	-67.2	-3.5	<i>h</i>	<i>h</i>
CN	-117.9	-118.0	-118.0	-0.1	<i>h</i>	<i>h</i>
<b>10</b>	-53.8 <sup>i</sup>	-53.4	<i>h</i>	<i>h</i>	<i>h</i>	<i>h</i>

<sup>a</sup> Solution data in  $\text{CDCl}_3$ . <sup>b</sup> Adsorbed on neutral  $\gamma\text{-Al}_2\text{O}_3$ . <sup>c</sup> Powdered crystalline solid. <sup>d</sup> Difference of B – A. <sup>e</sup> Adsorbed on acidic  $\gamma\text{-Al}_2\text{O}_3$ . <sup>f</sup> Adsorbed on basic  $\gamma\text{-Al}_2\text{O}_3$ . <sup>g</sup> Assignment according to ref 25. <sup>h</sup> Not measured. <sup>i</sup> Reference 25, adjusted to  $\text{CH}_3\text{NO}_2$  as standard.

alumina, on the other hand, yields, relative to the neat liquid, shifts of ca. 20 ppm for hydrogen bonding, 53 ppm for adsorption at Lewis acid sites, and 112 ppm for adsorption on Brønsted acid sites.<sup>13</sup> In our case, again only insignificant differences result if data from measurements on basic and acidic alumina are compared (Table 3). The pyrazole study mentioned above<sup>5</sup> came to the same conclusions with regard to the formation of protonated species.

## Conclusion

In conclusion, our results demonstrate that high-resolution  $^{19}\text{F}$  and  $^{15}\text{N}$  MAS NMR spectra of fluorinated and nitrogen-containing aromatics adsorbed on porous materials can be measured, even with nitrogen in natural abundance. The application of solution state NMR pulse sequences for assignment purposes thus becomes possible. With respect to the  $^{15}\text{N}$  CP/MAS NMR study of adsorbed pyrazole,<sup>5</sup> we mention that the use of pretreated porous materials with only small amounts of surface water (ca. 1%) reduces the NMR effect of line narrowing via adsorption.<sup>19</sup> In line with this observation, which indicates less mobility of the adsorbates due to access to strong adsorption sites which are most probably inactivated by surface water, is the fact that Aguilar-Parilla et al.<sup>5</sup> recorded  $^{15}\text{N}$  spectra using cross polarization. Clearly, this aspect needs further investigation. In the present study, the line widths were not optimized with respect to the water content of the adsorbent, but preliminary measurements<sup>19</sup> indicate that ca. 5% is usually enough to observe the described line-narrowing, higher concentrations being without significant further effect. For the  $^{19}\text{F}$  spectra discussed here, Figure 6 shows that thermal pretreatment of the adsorbent, which removes surface water and in addition alters the silica surface by formation of siloxane groups if temperatures above 400 °C are used,<sup>28</sup> has indeed a pronounced effect on the  $^{19}\text{F}$  NMR linewidths.

## Experimental Section

**Materials.** Compounds **1**, **8**, **9**, and **10** were purchased from Aldrich and used without further purification; **2** was available from earlier studies. The remaining systems were synthesized

(26) Duthaler, R. O.; Roberts, J. D. *J. Am. Chem. Soc.* **1978**, *100*, 4960.

(27) Städeli, W.; Philipsborn, W. v.; Wick, A.; Lichter, R. L. *Helv. Chim. Acta* **1980**, *63*, 504.

(28) Iler, R. K. *The Chemistry of Silica. Solubility, Polymerization, Colloid and Surface Properties and Biochemistry*; Wiley: New York, 1979.

**Table 4.**  $^{13}\text{C}$  Chemical Shift Data for **2**, **8**, and **9** and  $^1\text{H}$  Chemical Shift Data for **2** ( $\delta$ , ppm, relative to TMS)

<b>2</b>	C-1	C-2	C-3	C-4	C-5	C-6	C-7	C-8	
adsorb. <sup>a</sup>	130.3	115.1	161.5	107.4	122.6	126.3	126.9	128.5	
sol. <sup>b</sup>	131.78	116.31	162.48	108.53	123.96	127.60	128.17	129.41	
<b>2</b>	C-9	C-10	C-11	C-12	C-13	C-14			
adsorb. <sup>a</sup>	122.6	122.6	128.5	131.5	129.5	132.0			
sol. <sup>b</sup>	127.11	127.05	129.76	132.71	130.53	133.18			
<b>2</b>	1-H	2-H	4-H	5-H	6-H	7-H	8-H	9-H	10-H
sol. <sup>b</sup>	8.02	7.45	8.49	8.75	7.69	7.66	7.97	7.82	7.78
<b>8</b>	C-2	C-4	C-5,6,8	C-7	C-9	C-10			
adsorb. <sup>a</sup>	160.3	154.9	127.4	133.6	149.0	124.4			
cryst. <sup>c</sup>	160.4	155.3	128.2	132.9	148.5	124.9			
sol. <sup>d</sup>	160.7	155.9	127.6, 128.1, 128.6	134.4	150.3	125.4			
<b>9</b>	C-2	C-3	C-4	C-5,6,8	C-7	C-9	C-10	CN	
adsorb. <sup>a</sup>	149.7	106.1	141.6	128.5	133.0	147.7	125.5	117.4	
sol. <sup>b</sup>	150.6	107.2	142.5	129.4, 129.0, 130.2	133.4	149.3	126.9	117.8	

<sup>a</sup> Adsorbed on neutral  $\gamma\text{-Al}_2\text{O}_3$ . <sup>b</sup> Solution data, this work. <sup>c</sup> Crystalline powder. <sup>d</sup> Solution data from ref 35.

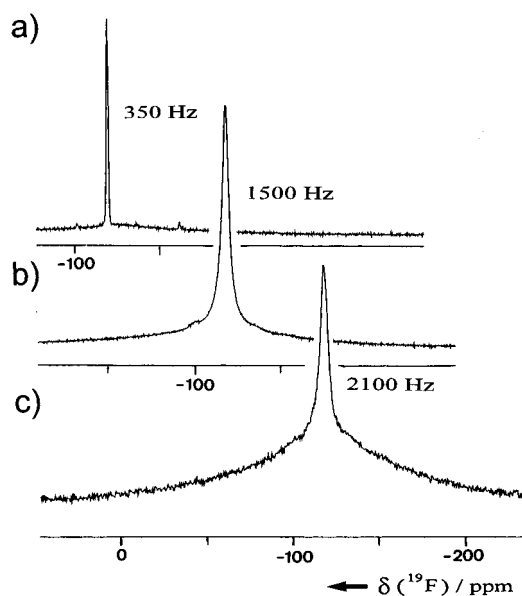


**Figure 6.** 282.4 MHz  $^{19}\text{F}$  MAS NMR spectra of 1-fluoroanthracene (**3**) on silica 60, without  $^1\text{H}$  decoupling, mass ratio 1:6, rotational frequency 5 kHz; (a) no thermal pretreatment, 4.6% surface water; (b) 6 h at 250 °C and  $10^{-6}$  Torr, 0% surface water by thermogravimetric measurement; (c) 6 h at 900 °C and  $10^{-6}$  Torr;  $\delta(^{19}\text{F}) = -119.2$  ppm relative to  $\text{C}^{19}\text{FCl}_3$ ; line widths at half-height as given.

according to the literature: **3**,<sup>29,30</sup> **4**,<sup>30,31</sup> **5**,<sup>32</sup> **6**,<sup>29</sup> **7**.<sup>29</sup> Silica 60 was a product of Merck KGaA, Darmstadt, Germany (product No. 7733) for column chromatography, particle size 200–500  $\mu\text{m}$  (35–70 mesh ASTM), specific surface area (BET) 370  $\text{m}^2/\text{g}$ , mean pore diameter 6 nm;  $\gamma$ -alumina 90 neutral, acidic, and basic were products of Woelm-Pharma, Eschwege, Germany, activation grade I for column chromatography, particle size 50–200  $\mu\text{m}$  (70–290 mesh ASTM). For sample preparation, weighed amounts of organic compound and adsorbent were mixed and ground in an agate mortar for ca. 5 min. For the thermogravimetric measurements a TG50 sample cell (Mettler) and the Graphware TA72 program (Mettler) were used.

(29) Valkanas, G.; Hopf, H. *J. Org. Chem.* **1962**, *27*, 3680.

(30) Martin, E. L. *J. Org. Chem.* **1936**, *58*, 1438.

(31) Bergmann, E. D.; Blum, J.; Butanara, S. *J. Org. Chem.* **1961**, *26*, 3211.

(32) Dewar, M. J. S.; Michl, J. *Tetrahedron* **1970**, *26*, 375.

**Spectra.** Solid state MAS NMR spectra were recorded with a Bruker MSL 300 spectrometer, operating at a  $^1\text{H}$  frequency of 300.1 MHz and  $^{13}\text{C}$ ,  $^{15}\text{N}$ , and  $^{19}\text{F}$  frequencies of 75.5, 30.4, and 282.4 MHz, respectively.  $\text{ZrO}_2$  rotors with 4 mm ( $^{13}\text{C}$ ,  $^{19}\text{F}$ ) and 7 mm ( $^{15}\text{N}$ ) o.d. and Kel-F caps were used. Temperature readings from the Bruker variable temperature unit for measurements above rt were not corrected for possible frictional heating due to MAS. For the  $^{19}\text{F}$  measurements, the  $^1\text{H}$  decoupler coil of a broadband MAS probehead was tuned to the  $^{19}\text{F}$  frequency;  $^1\text{H}$  decoupling (decoupler field 70 kHz) was thus used only for the  $^{13}\text{C}$  and  $^{15}\text{N}$  MAS spectra, where the decoupler was on during acquisition. The chemical shifts were measured with respect to the spectrometer reference frequency which was calibrated for the  $^{19}\text{F}$  measurements against the signal of liquid  $\text{C}_6\text{F}_6$  with  $-163$  ppm<sup>33</sup> on the  $^{19}\text{F}$  chemical shift scale relative to  $\delta(\text{C}^{19}\text{FCl}_3) = 0.0$  ppm. The data from the solution measurements in acetone- $d_6$  and  $\text{CDCl}_3$ , performed with a Bruker AMX 400 spectrometer, were corrected for volume susceptibility effects. Similar corrections for the solid state MAS spectra of the adsorbed species were not applied, because calculations based on the work of Michel et al.<sup>34</sup> showed that the effects are smaller than the experimental error ( $< 0.5$  ppm) achieved in our measurements. For  $^{13}\text{C}$ , a similar referencing procedure was based on the  $\text{CH}_2$  resonance of adamantane ( $\delta_{\text{TMS}} = 38.4$  ppm<sup>35</sup>), and for  $^{15}\text{N}$  on liquid  $\text{CH}_3\text{NO}_2$  with  $\delta(^{15}\text{N}) = 0.0$  ppm (see above). Individual spectra were run with typically 700–3000 transients and a relaxation delay of 3 or 5 s. Other details are given in the figure legends. The  $^{13}\text{C}$  data for **2**, **8**, and **9** are collected in Table 4. *Spectral assignments* for the  $^{19}\text{F}$  resonances in **1** followed from the  $^{19}\text{F}$ ,  $^{19}\text{F}$  COSY spectrum and formed in turn the basis for the  $^{13}\text{C}$  assignment by the  $^{13}\text{C}$ ,  $^{19}\text{F}$  HETCOR spectrum.<sup>36</sup> The more elaborate assignment of the  $^1\text{H}$  NMR spectrum of **2** was obtained in solution (data see Table 4) and started with a  $J$ -resolved 2D  $^1\text{H}$  spectrum<sup>37</sup> which differentiated between homonuclear  $^1\text{H}$ ,  $^1\text{H}$  and heteronuclear  $^1\text{H}$ ,  $^{19}\text{F}$  coupling constants. This allowed an assignment of  $\delta(4\text{-H})$  and  $\delta(5\text{-H})$  with the latter at lowest field and not coupled to the fluorine in the 3-position. A COSY-45 experiment<sup>38</sup> yielded

(33) Mann, B. E. *NMR and the Periodic Table*; Harris R. K., Mann, B. E., Eds.; Academic Press: London 1978; p 99.

(34) Michel, D.; Meiler, W.; Gutsze, A.; Wronkowski, A. *Z. Phys. Chem. (Leipzig)* **1980**, *261*, 953.

(35) Kalinowski, H. O.; Berger, S.; Braun, S.  *$^{13}\text{C}$  NMR Spektroskopie*; Thieme: Stuttgart, 1984; p 356.

(36) HETCOR  $^{13}\text{C}$ ,  $^{19}\text{F}$  correlations have also been reported by Ribeiro and Glen (Ribeiro, A. A.; Glen, M. J. *J. Magn. Reson., Ser. A* **1994**, *107*, 158) and a  $^{19}\text{F}$  detected  $^{13}\text{C}$ ,  $^{19}\text{F}$  HMQC experiment was described by Berger (Berger, S. *J. Fluorine Chem.* **1995**, *72*, 117).

(37) Aue, W. P.; Karhan, J.; Ernst, R. R. *J. Chem. Phys.* **1976**, *64*, 4226.

(38) Bax, A.; Freeman, R. *J. Magn. Reson.* **1981**, *44*, 542.

the remaining proton assignments which were in turn used to derive the  $^{13}\text{C}$  assignment via gradient-enhanced HMQC<sup>39</sup> and HMBC<sup>40</sup> experiments, the latter improved by the introduction of a low-pass filter.<sup>41</sup> The assignment of the  $^1\text{H}$  and  $^{13}\text{C}$  resonances of **9** followed from COSY-45<sup>38</sup> and HETCOR spectra,<sup>42</sup> the latter optimized for one-bond and long-range  $^{13}\text{C},^1\text{H}$  coupling.

---

(39) Hurd, R. E.; John, B. K. *J. Magn. Reson.* **1991**, *91*, 468.

(40) Wilker, W.; Leibfritz, D.; Kerssebaum, R.; Bermel, W. *Magn. Reson. Chem.* **1993**, *31*, 287.

(41) Kogler, H.; Sørensen, O. W.; Bodenhausen, G.; Ernst, R. R. *J. Magn. Reson.* **1983**, *55*, 157.

**Acknowledgment.** We are indebted Professor Dr. D. Michel, Leipzig, and Dr. S. Oepen, Siegen, for helpful discussions and to the Volkswagen-Stiftung for a spectrometer grant. Financial support by the Fonds der Chemischen Industrie, Frankfurt/M., is gratefully acknowledged.

JO961104O

---

(42) Maudsley, A. A.; Müller, L.; Ernst, R. R. *J. Magn. Reson.* **1977**, *28*, 463. Bodenhausen, G.; Freeman, R. *J. Magn. Reson.* **1977**, *28*, 471.